A Time-Delayed Hyperchaotic System Composed of Multiscroll Attractors With Multiple Positive Lyapunov Exponents

Yue Wang
College of Computer Science and Electronic Engineering,
Hunan University,
Changsha 410082, China
e-mail: yuewang@hnu.edu.cn

Chunhua Wang[1]
College of Computer Science and Electronic Engineering,
Hunan University,
Changsha 410082, China
e-mail: wch1227164@hnu.edu.cn

Ling Zhou
College of Computer Science and Electronic Engineering,
Hunan University,
Changsha 410082, China
e-mail: zhouling0340@163.com

The paper proposes a time-delayed hyperchaotic system composed of multiscroll attractors with multiple positive Lyapunov exponents (LEs), which are described by a three-order nonlinear retarded type delay differential equation (DDE). The dynamical characteristics of the time-delayed system are far more complicated than those of the original system without time delay. The three-order time-delayed system not only generates hyperchaotic attractors with multiscroll but also has multiple positive LEs. We observe that the number of positive LEs increases with increasing time delay. Through numerical simulations, the time-delayed system exhibits a larger number of scrolls than the original system without time delay. Moreover, different numbers of scrolls with variable delay and coexistence of multiple attractors with a variable number of scrolls are also observed in the time-delayed system. Finally, we setup electronic circuit of the proposed system, and make Pspice simulations to it. The Pspice simulation results agree well with the numerical results. [DOI: 10.1115/1.4036831]

Keywords: hyperchaotic, multiscroll, time delay, Lyapunov exponents, electronic circuit

1 Introduction

For the last few decades, the study on delay dynamical systems has been considered one of the most important fields of research owing to its ubiquity in various fields including biology, physics, mathematics, engineering, etc. [1]. DDEs have been successfully used to model natural systems which contain one or more time delays, such as blood production in patients with leukemia (Macky–Glass (MG) model), physiological model, population dynamics, control system, and neural networks [2].

Beyond the mathematical modeling of the naturally occurring phenomena, time-delayed systems have been extensively studied in the literature for some important reasons, such as: (i) in the networks of coupled neurons, time delay has been shown to affect the enhancement or suppression of synchronized oscillations, amplitude death, and phase-coherent dynamic behaviors, etc. [3]. In particular, in the network of nonlinear oscillators, signal transmission time delays are known to be responsible for many interesting dynamic behaviors including phase-flip transitions leading to synchrony or out of synchrony [3]. (ii) Time delay makes a system infinite dimensional and enforces it to produce chaos with higher dimensionality, which cannot be obtained from a low-dimensional system [4]. Especially, the infinite dimensionality of the time-delayed system offers an opportunity to enhance the richness of hyperchaos, having multiple positive LEs. Therefore, time-delayed systems with multiple positive LEs have been identified as great candidates to improve the security in the communication schemes [5]. Apart from secure communication, chaotic and hyperchaotic systems also play important roles in cryptography [6] and chaos-based noise generators [7], etc.

For the above-mentioned reasons, researchers have carried out extensive studies of time-delayed systems, which can generate one or more positive LEs. Since Mackey and Glass proposed the first chaotic delay differential equation which is a model of blood production in patients with leukemia in 1977, various delay chaotic systems have been reported [1,2,8–10]. By using feedback controller or threshold controller, some chaotic oscillations with time delay have been proposed, which exhibit chaotic attractors with mono-scroll or double-scroll [8,9]. Tamaševičius and Pyragiene introduced a N-shaped nonlinear function in delay dynamical system instead of commonly used Mackey–Glass type function to exhibit hyperchaotic attractors with two-scroll [10]. Biswas and Banerjee reported the design, analysis, and experimental implementation of two first-order time-delayed dynamical systems which have different nonlinear functions, and in these systems both chaotic and hyperchaotic attractors with monoscroll and double-scroll can be observed [1,2].

However, in the above literatures, time-delayed chaotic or hyperchaotic systems only generate monoscroll or double-scroll attractors, and they do not generate multiscroll attractors. Generally speaking, dynamical systems with multiscroll attractors can present more complex dynamics than general chaotic system with monoscroll or double-scroll. Although many methods have been proposed to generate multiscroll attractors [11–17], such as methods of piecewise linear function, saturated function, trigonometric function, absolute value function, polynomial function, hyperbolic function, modulation function, sign function, and nonlinear hysteresis function. Nevertheless, these methods can only construct chaotic or hyperchaotic systems with multiscroll attractors, having one or two positive LEs.

In this paper, we propose a time-delayed hyperchaotic system composed of multiscroll attractors. The time-delayed system can not only generate multiscroll attractors but also has multiple positive LEs. This is the main advantage of the proposed system over the previous ones. We carry out stability analysis to identify the parameter zone for which the system shows a stable equilibrium response. Then, the proposed time-delayed system is simulated numerically. The system dynamics is characterized with LEs spectrum and bifurcation diagram. With the variation of time delay and other system parameters, the system shows a lot of dynamical behaviors, such as Hopf bifurcation, a period doubling route to chaos, and hyperchaos with multiple positive LEs. Through the phase diagram, we can observe hyperchaotic attractors with multiscroll and coexistence of multiple attractors with a variable number of scrolls, etc. Finally, the time-delayed system

[1]Corresponding author.

Contributed by the Design Engineering Division of ASME for publication in the Journal of Computational and Nonlinear Dynamics. Manuscript received February 27, 2017; final manuscript received May 10, 2017; published online July 12, 2017. Assoc. Editor: Zaihua Wang.

has been realized by electronic circuit, and Pspice simulations are made. We plot the phase diagram of the system, and the circuit simulation results agree well with the numerical results.

The paper is organized in the following way: Section 2 proposes the time-delayed system and reports its stability analysis. Section 3 reports the numerical simulations including Lyapunov exponents, bifurcation diagram, and phase diagram. Section 4 reports the electronic circuit realization and Pspice simulations of the system. Section 5 concludes the outcome of the whole work.

2 The Proposed System and Its Stability Analysis

Let us consider the following three-order system proposed by Sprott [18,19]:

$$\begin{cases} \dot{x} = y \\ \dot{y} = z \\ \dot{z} = -ay - az + af(x) \end{cases} \tag{1}$$

which is often called the jerk system. The dynamical characteristics of the system (1) are dependent on the selection of $f(x)$.

In Ref. [20], the form of a periodic function is described by

$$f(x) = \sin(2\pi bx) \tag{2}$$

and multiscroll attractors can be generated in the system (1) when we select Eq. (2) as $f(x)$. The jerk system with multiscroll attractors can be written as follows:

$$\begin{cases} \dot{x} = y \\ \dot{y} = z \\ \dot{z} = -ay - az + a\sin(2\pi bx) \end{cases} \tag{3}$$

where $a, b \in R^+$.

If we introduce time delay into the system (3), the proposed three-order time-delayed system can be obtained as follows:

$$\begin{cases} \dot{x} = y(t-\tau) \\ \dot{y} = z \\ \dot{z} = -ay - az + a\sin(2\pi bx) \end{cases} \tag{4}$$

where $\tau \in R^+$ is the intrinsic time delay in the time-delayed system (4).

2.1 Stability of Fixed Point. The equilibrium points of the time-delayed system (4) can be obtained by solving the following equations:

$$\begin{cases} y(t-\tau) = 0 \\ z = 0 \\ -ay - az + a\sin(2\pi bx) = 0 \end{cases} \tag{5}$$

where $y(t-\tau) = y$. We can easily observe that the time-delayed system (4) has infinitely many equilibria $O = \{(x, y, z) \mid x = n/2b, y = z = 0\}$, where $n = 0, 1, 2, 3, 4, \ldots$. By linearizing the time-delayed system (4) at point O, we can obtain the Jacobian matrix

$$\mathrm{Jo} = \begin{pmatrix} 0 & e^{-\lambda\tau} & 0 \\ 0 & 0 & 1 \\ \pm 2\pi ab & -a & -a \end{pmatrix} \tag{6}$$

According to Eq. (6), the characteristic equation is given by

$$\lambda^3 + a\lambda^2 + a\lambda + re^{-\lambda\tau} = 0 \tag{7}$$

where $r = \pm 2\pi ab$.

2.1.1 Stability for $\tau = 0$. At $\tau = 0$, the characteristic equation (7) reduces to

$$\lambda^3 + a\lambda^2 + a\lambda + r = 0 \tag{8}$$

Asymptotic stability will occur when all the roots of the characteristic equation have negative real parts. By the Routh–Hurwitz criterion, all roots of Eq. (8) have negative real parts if and only if

$$a > 0, \quad r > 0, \quad a^2 - r > 0 \tag{9}$$

Equation (9) is the first condition for choosing the system parameters to achieve asymptotic stability of the time-delayed system (4) for $\tau = 0$.

2.1.2 Stability for $\tau \neq 0$. Hopf bifurcation will appear if at least one of the eigenvalues crosses the imaginary axis from the left and enters the right half-plane. Thus, if the real part of eigenvalue varies from the left to right, we can say that the real part which is less than zero is a stable state, the real part which is greater than zero is a bifurcated state, and the real part which is equal to zero is the limiting case. At the emergence of Hopf bifurcation, we make the real part be equal to zero.

Clearly, $i\omega$ $(\omega > 0)$ is a root of Eq. (7) if and only if

$$-i\omega^3 - a\omega^2 + ia\omega + r(\cos\omega\tau - i\sin\omega\tau) = 0 \tag{10}$$

Separating the real and imaginary parts, we have

$$\begin{cases} a\omega^2 = r\cos\omega\tau \\ -\omega^3 + a\omega = r\sin\omega\tau \end{cases} \tag{11}$$

Adding up the squares of both equations, we obtain

$$\omega^6 + (a^2 - 2a)\omega^4 + a^2\omega^2 - r^2 = 0 \tag{12}$$

Let $z = \omega^2$ and denote $p = a^2 - 2a$, $q = a^2$, and $v = -r^2$. Then, Eq. (12) becomes

$$z^3 + pz^2 + qz + v = 0 \tag{13}$$

Denote

$$h(z) = z^3 + pz^2 + qz + v \tag{14}$$

Then

$$h'(z) = 3z^2 + 2pz + q \tag{15}$$

Clearly, $h(0) = v < 0$, and $\lim_{z\to\infty} h(z) = \infty$. Hence, there exists a $z_0 \in (0, \infty)$ so that $h(z_0) = 0$. Thus, Eq. (13) has at least one positive root. Without the loss of generality, we suppose that Eq. (13) has three positive roots, denoted by z_1, z_2, and z_3, respectively. Then, Eq. (12) has three positive roots, say

$$\omega_1 = \sqrt{z_1}, \quad \omega_2 = \sqrt{z_2}, \quad \omega_3 = \sqrt{z_3}$$

Let

$$\tau_k^{(j)} = \frac{1}{\omega_k}\left[\arcsin\left(-\frac{\omega_k^3 - a\omega_k}{r}\right) + 2(j-1)\pi\right], k = 1,2,3; j = 1,2,\ldots \tag{16}$$

Then, $\pm i\omega_k$ is a pair of purely imaginary roots of Eq. (7) with $\tau = \tau_k^{(j)}$; $k = 1, 2, 3$; $j = 1, 2, \ldots$. Clearly

$$\lim_{j\to\infty} \tau_k^{(j)} = \infty, \quad k = 1, 2, 3$$

According to the Hopf analysis in Ref. [21], it has some necessary definitions, such as τ_0 and $\lambda(\tau)$, and there we use the same definitions

$$\tau_0 = \tau_{k_0}^{(j_0)} = \min_{1\le k\le 3, j\ge 1}\left\{\tau_k^{(j)}\right\}, \omega_0 = \omega_{k_0} \tag{17}$$

Let

$$\lambda(\tau) = \alpha(\tau) + i\omega(\tau) \tag{18}$$

the root of Eq. (7) satisfying

$$\alpha(\tau_0) = 0, \quad \omega(\tau_0) = \omega_0$$

Differentiating both sides of Eq. (7) with respect to τ gives

$$\frac{d\lambda(\tau)}{d\tau} = \frac{r\lambda e^{-\lambda\tau}}{3\lambda^2 + 2a\lambda + a - r\tau e^{-\lambda\tau}}$$

It follows from Eq. (7) that:

$$\frac{d\mathrm{Re}\lambda(\tau_0)}{d\tau} = \frac{w_0^2}{\Delta}\left[3\omega_0^4 + 2(a^2 - 2a)\omega_0^2 + a^2\right]$$

where

$$\Delta = \left(3\omega_0^2 - a + r\tau_0\cos\omega_0\tau_0\right)^2 + \left(2a\omega_0 + r\tau_0\sin\omega_0\tau_0\right)^2$$

Let ω_0, τ_0, and $\lambda(\tau)$ be defined by Eqs. (17) and (18), respectively, and $z_0 = {\omega_0}^2$. Suppose that $a > 0$, $r > 0$, $a^2 - r > 0$. According to the Theorem 2.4 in Ref. [21], then

(i) Because $v < 0$, all roots of Eq. (7) have negative real parts when $\tau \in [0, \tau_0)$.
(ii) Because $v < 0$, when $\tau = \tau_0$ and $h'(z_0) \neq 0$, $\pm i\omega_0$ is a pair of simple purely imaginary roots of Eq. (7) and all other roots have negative real parts. Moreover, when $\tau \in (\tau_0, \tau_1)$, $d\mathrm{Re}\lambda(\tau_0)/d\tau > 0$, and Eq. (7) has at least one root with a positive real part, where τ_1 is the first value of $\tau > \tau_0$ such that Eq. (7) has purely imaginary root.

According to the Theorem 11.1 in Ref. [22] and the analysis of the preceding context, we conclude that

(i) Because $v < 0$, when $\tau \in [0, \tau_0)$, equilibrium points of the time-delayed system (4) are locally asymptotically stable.
(ii) Because $v < 0$, when $\tau = \tau_0$ and $h'(z_0) \neq 0$, system (4) exists Hopf bifurcation at its equilibrium points.

3 Numerical Simulations

3.1 Lyapunov Exponents. We calculate LEs of the time-delayed system (4) with a method similar to the one described by Farmer [23], which is essentially the method described by Benettin et al. [24]. However, there is a crucial change to adapt the Shampine–Thompson approach [25] which is based on the Bogacki–Shampine Runge–Kutta method, namely, for purposes of obtaining the norms of tangent vectors and applying the Gram–Schmidt orthonormalization, a function scalar product is used.

The spectrum of LEs in the τ parameter space are calculated by setting $a = 1.2$, $b = 8$ of the time-delayed system (4), which is shown in Fig. 1(*a*). It is obvious from Fig. 1(*a*) that the time-delayed system (4) has four positive LEs for $\tau \in [5.6, 8]$, while it has three positive LEs for $\tau \in [3.55, 5.55]$. It has two positive LEs for $\tau \in [1.5, 3.5]$, and the system (4) has one positive LEs for $\tau \in [0.05, 1.5]$.

To compare the dynamical complexity of the time-delayed system (4) and the nontime-delayed system (3), we calculate LEs of the two systems with variable b which are shown in Figs. 1(*b*) and 1(*c*). It is obvious from Figs. 1(*b*) and 1(*c*) that the time-delayed system (4) has four positive LEs with variable b when $a = 1.2$ and $\tau = 8$, while the nontime-delayed system (3) has only one positive LEs with variable b when parameter a is the same.

By setting the system parameters as $a = 1.2$, $b = 8$ and $\tau = 1.5$, hyperchaotic attractors of the time-delayed system (4) are plotted in Figs. 2(*a*) and 2(*b*). Figure 2(*b*) denotes the local amplification of (*a*). It is obvious from Figs. 1(*a*) and 2(*b*) that the time-delayed system (4) has hyperchaotic attractors with multiscroll when system parameters are chosen properly.

3.2 Bifurcation Diagrams. Bifurcation diagrams of the time-delayed system (4) with τ as the control parameter are shown in Figs. 3(*a*) and 3(*b*), which are obtained by plotting the local maxima of y. Figure 3(*b*) denotes the local amplification of (*a*). According to the analysis of bifurcation and periodic orbit in Refs. [2] and [26], the system (4) can be analyzed further more. When the system parameters are set to $a = 1.2$, $b = 0.15$, and initial conditions $(x(0), y(0), z(0)) = (1, 0, 0)$ in this section, we have $\tau_0 = 0.255$ from Eqs. (16) and (17). Thus, we expect that at $\tau_0 = \tau_H = 0.255$, the fixed point loses its stability through Hopf bifurcation, which is in accordance with the bifurcation diagram of Fig. 3(*a*). From Figs. 3(*a*) and 3(*b*), the system (4) shows a period doubling route to chaos beginning with $\tau = 2.1$. At $\tau = 2.77$, period-1 orbit becomes unstable and period-2 orbit appears. Further period doubling occurs at $\tau = 2.88$. Through a period doubling sequence, the system enters into the chaotic regime at $\tau = 2.95$. With future increase of τ, at $\tau = 7.1$, the system shows the emergence of hyperchaos.

We compute the first six Lyapunov exponents in the τ parameter space, which is shown in Fig. 3(*c*). It agrees well with the bifurcation diagrams. A phase plane representation in the x–y plane for different τ is shown in Figs. 3(*d*)–3(*f*), which shows the following characteristics: period-1 ($\tau = 2.7$), period-2 ($\tau = 2.8$), and period-4 ($\tau = 2.9$).

3.3 More Scrolls in the Time-Delayed System (4) Than the Ones in the Nontime-Delayed System (3). Both the nontime-delayed system (3) and the time-delayed system (4) can generate multiscroll attractors when parameters a and b are chosen properly. For simplicity, to induce and keep a chaotic state with multiscroll attractors in systems (3) and (4), parameters are selected as $a = 0.3$ and $b = 0.25$. The numerical results in Fig. 4 show that the nontime-delayed system (3) and the time-delayed system (4) generate different numbers of scrolls when the simulation time is the same, and more scrolls can be observed in the time-delayed system (4) than the ones in the nontime-delayed system (3) when the simulation time is 3000.

3.4 Different Numbers of Scrolls With Variable τ. The multiscroll attractors of the time-delayed system (4) using different choices of τ are plotted in Fig. 5, and the system parameters are selected as $a = 0.3$, $b = 0.25$. It is obvious from Fig. 5 that the system (4) has 13 scrolls when $\tau = 0.1$, while it has more than 20 scrolls when $\tau = 0.5$. The numbers of scrolls in the system (4) are different when τ varies in the interval [0.1, 0.5].

3.5 Coexistence of Multiple Attractors With a Variable Number of Scrolls. Coexistence of multiple attractors are two or more attractors in a system with the same parameter but different initial conditions [27]. Coexistence of multiple attractors means that dynamical characteristics of nonlinear systems are sensitive to the changes of initial conditions. It is well known that such a phenomenon may induce many special effects such as symmetry-breaking bifurcation, symmetry-restoring crisis, coexisting bifurcations, and hysteresis [28]. The multiscroll attractors of the time-delayed system (4) using the different choices of initial conditions are plotted in Fig. 6, and the system parameters are selected as $a = 0.3$, $b = 0.25$. Coexistence of multiple attractors with a variable number of scrolls can be observed in the time-delayed system (4). It is obvious from Fig. 6 that the time-delayed

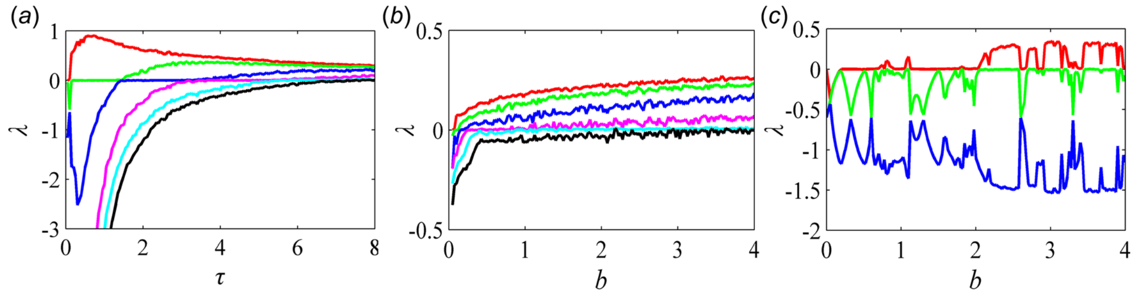

Fig. 1 LEs of the nontime-delayed system (3) and time-delayed system (4) when initial conditions (x(0), y(0), z(0)) = (1, 1, 1): (*a*) LEs of the system (4), (*b*) LEs of the system (4), and (*c*) LEs of the system (3)

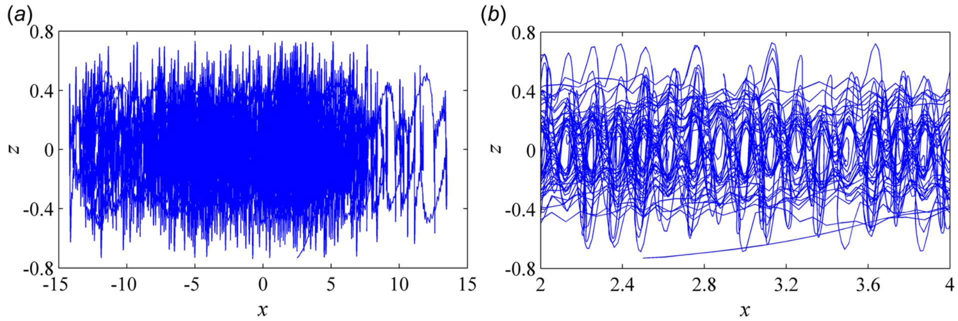

Fig. 2 Hyperchaotic attractors with multiscroll of the time-delayed system (4) when t = 3000 and initial conditions (x(0), y(0), z(0)) = (1, 1, 1): (*a*) hyperchaotic attractors and (*b*) local amplification of (*a*)

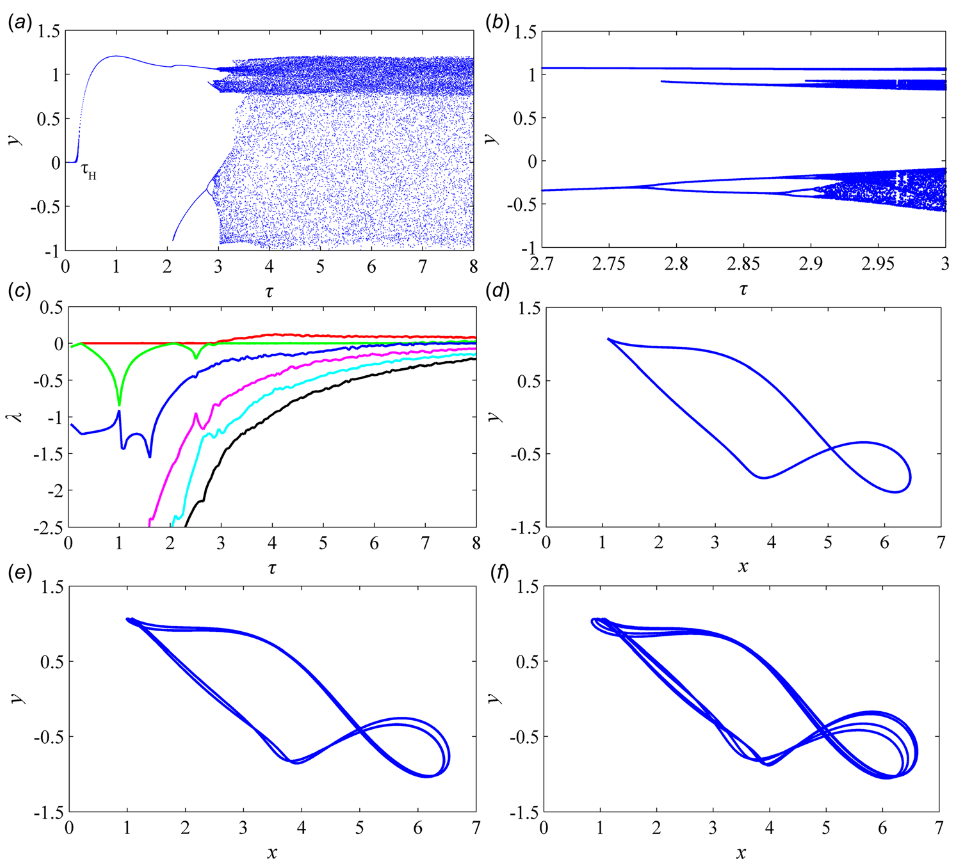

Fig. 3 Bifurcation diagram, LEs and x–y phase plane of the time-delayed system (4): (*a*) bifurcation diagram, (*b*) local amplification of (*a*), (*c*) LEs diagram, (*d*) x–y phase plane for τ = 2.7 (period-1), (*e*) x–y phase plane for τ = 2.8 (period-2), and (*f*) x–y phase plane for τ = 2.9 (period-4)

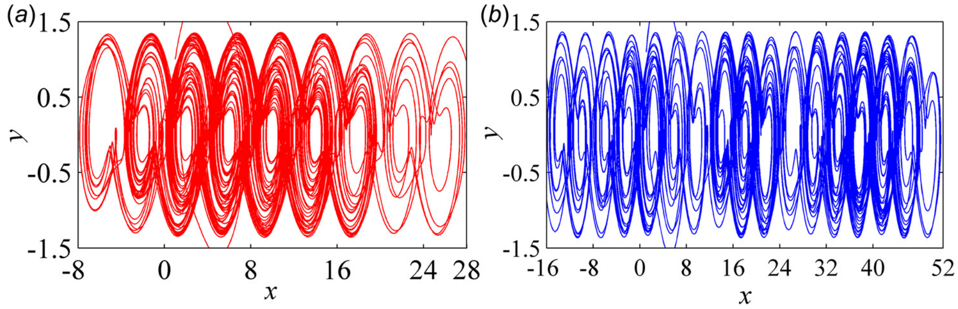

Fig. 4 Multiscroll attractors of the nontime-delayed system (3) and the time-delayed system (4) when initial conditions (*x*(0), *y*(0), *z*(0)) = (1, 1, 1): (*a*) system (3) and (*b*) system (4) with $\tau = 0.1$

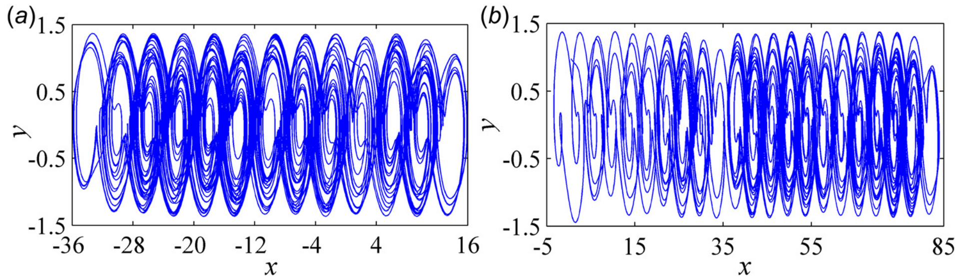

Fig. 5 Different numbers of scrolls of the time-delayed system (4) when initial conditions (*x*(0), *y*(0), *z*(0)) = (0, 1, 0) and *t* = 3000: (*a*) $\tau = 0.1$ and (*b*) $\tau = 0.5$

system (4) has 11-scroll attractors within x varying in the interval $[-8, 36]$ for initial conditions $(x(0), y(0), z(0)) = (0, 0, 1)$, while it has 13-scroll attractors within x varying in the interval $[-36, 16]$ for initial conditions $(x(0), y(0), z(0)) = (0, 1, 0)$.

4 Electronic Circuit Realization and Its Simulations

The proposed time-delayed system (4) is realized by the electronic circuit which is shown in Fig. 7, and we make Pspice simulations to it. According to Kirchhoff circuit laws, the circuit equation of the system (4) can be written as follows:

$$\begin{cases} (R_{15}C_4)dx/dt = \dfrac{R_{16}}{R_1} y_\tau \\ (R_{19}C_5)dy/dt = \dfrac{R_{20}}{R_{21}} z \\ (R_{24}C_6)dz/dt = R_{25}\left(-\dfrac{y}{R_{26}} - \dfrac{z}{R_{27}} + \dfrac{\sin(Gx)}{R_{28}}\right) \end{cases} \tag{19}$$

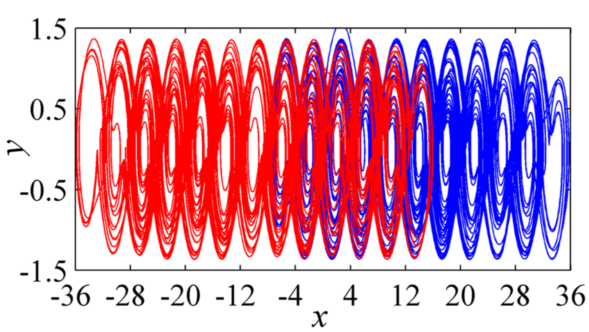

Fig. 6 Coexistence of multiple attractors of the time-delayed system (4) when $\tau = 0.1$ and *t* = 3000: *x* varying in the interval [−8, 36] for initial conditions (*x*(0), *y*(0), *z*(0)) = (0, 0, 1) and the interval [−36, 16] for initial conditions (*x*(0), *y*(0), *z*(0)) = (0, 1, 0)

to Eq. (19), the integrator, adder, and phase inverter can be realized by the use of operational amplifiers. A sine signal generator which is obtained from the Pspice component library can realize the nonlinear function [29]. Different choices of R_{25} and gain (G) of Eq. (19) can realize the changes of parameter a and b of the time-delayed system (4), respectively. Equation (19) can be equivalent to the time-delayed system (4) with parameter $a = 0.3$ and $b = 0.25$ when the resistance values are selected as $R_{16} = R_{20} = R_{25} = R_1 = R_{21} = 10$ kΩ, $R_{26} = R_{27} = R_{28} = 33$ kΩ, $R_{29} = 8$ kΩ, and $G = 1.57$. The integration time constant of the integrator is $R_{24}C_6$, and different values of R_{24} or C_6 can change the frequency range. We select $R_{15} = R_{19} = R_{24} = 50$ kΩ and $C_4 = C_5 = C_6 = 20\,\mu$F in the Pspice simulations of the circuit equation (19).

The time delay is realized by an active first-order all pass filter (APF) which is shown in Fig. 8 [1]. The APF is designed with the following parameters: $R_{30} = R_{31} = 2.2$ kΩ, $R = 10$ kΩ, and $C = 10$ nF. Because that each APF contributes a delay of $T_d \approx RC = 0.1$ ms, the dimensionless parameter $\tau = RC/R_0C_0 = 1$. If one wants to produce a delay $\tau = i$, i blocks are needed. We get variable time delays by varying R.

4.1 Hyperchaotic Attractors With Multiscroll. We change the system parameters of the time-delayed system (4) to $a = 1.2$ and $b = 8$ by setting $R_{25} = 40$ kΩ and $G = 50$. The $\tau = 1.5$ is obtained by using two stages of APF with $R = 10$ kΩ and $R = 5$ kΩ, respectively. According to these changes of electronic circuit parameters, Pspice simulations are made to the time-delayed system (4). It is obvious from Figs. 1 and 9 that hyperchaotic attractors with multiscroll can be obtained when system parameters are chosen properly.

4.2 More Scrolls in the Time-Delayed System (4) Than the Ones in the Nontime-Delayed System (3). To confirm the time-delayed system (4) which can generate more scrolls than the nontime-delayed system (3) when the system parameters are selected as $a = 0.3$, $b = 0.25$, we set $R_{25} = 10$ kΩ and $G = 1.57$. The $\tau = 0.1$ of the time-delayed system (4) is obtained by using

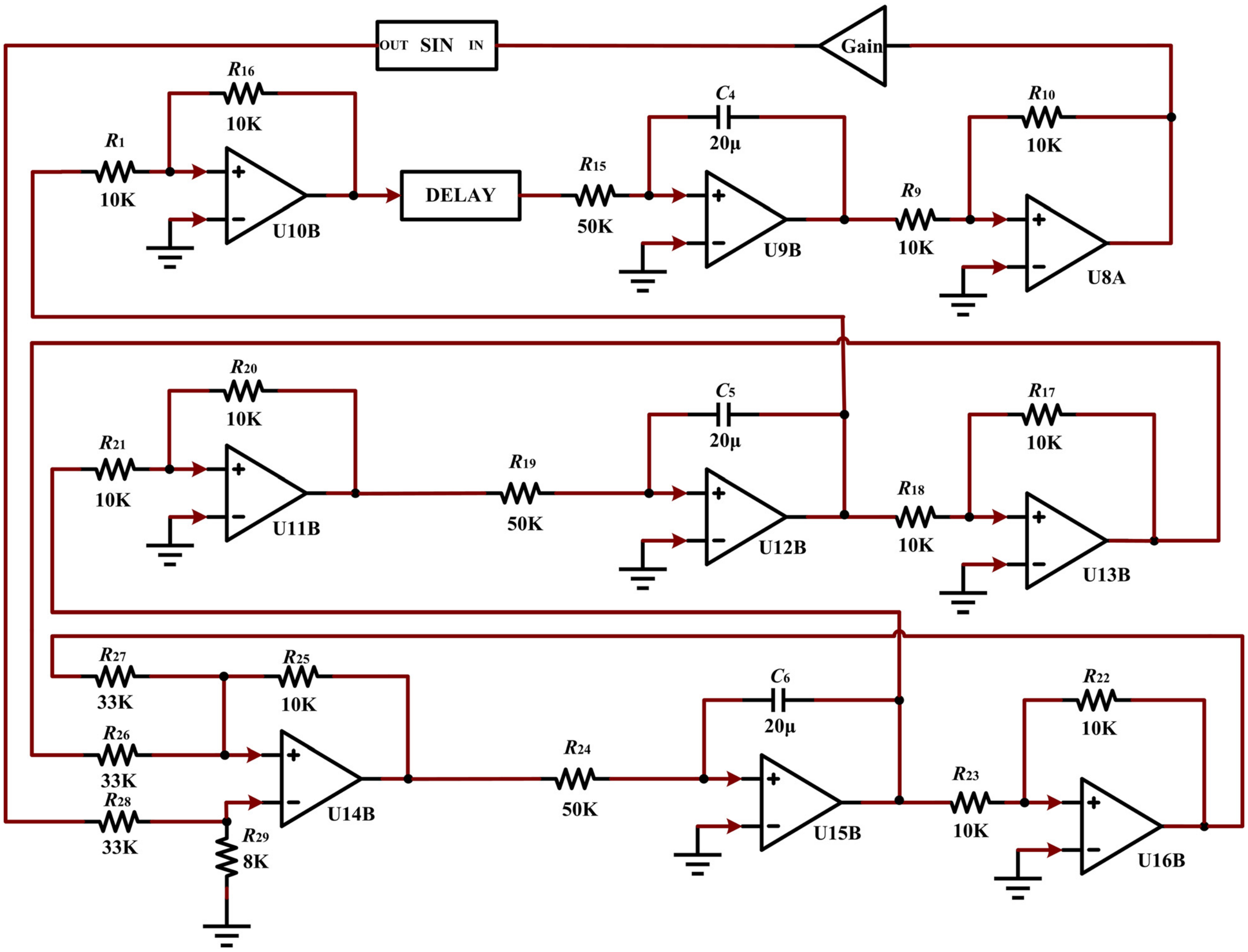

Fig. 7 The electric circuit realization of the time-delayed system (4)

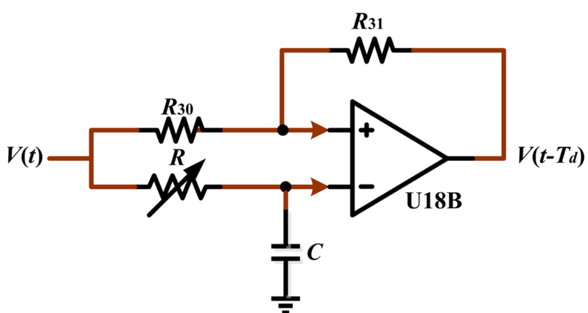

Fig. 8 Active first-order all pass filter: $R_{30} = R_{31} = 2.2$ kΩ and $C = 10$ nF

one APF with $R = 1$ kΩ. The electric circuit realization of the nontime-delayed system (3) can be obtained by removing delay of Fig. 7. According to these electronic circuit parameters, Pspice simulations are made to systems (3) and (4). It is obvious from Fig. 10 that more scrolls can be observed in the time-delayed system (4) than the ones in the nontime-delayed system (3) when the simulation time is 3000.

4.3 Different Numbers of Scrolls With Variable τ. We fix the system parameters of the time-delayed system (4) to $a = 0.3$ and $b = 0.25$ by setting $R_{25} = 10$ kΩ and $G = 1.57$, and we vary the intrinsic time delay τ. The $\tau = 0.1$ is obtained by using only one APF with $R = 1$ kΩ, and $\tau = 0.5$ is obtained by setting $R = 5$ kΩ. According to the changes of R, Pspice simulations are made to the time-delayed system (4). It is obvious from Fig. 11 that the time-delayed system (4) has 13 scrolls when $\tau = 0.1$, while it has more than 20 scrolls when $\tau = 0.5$. The numbers of scrolls of the time-delayed system (4) are different when τ varies in the interval [0.1, 0.5].

4.4 Coexistence of Multiple Attractors With a Variable Number of Scrolls. The circuit simulation results of the time-delayed system (4) using the different choices of initial conditions are plotted in Fig. 12. The system parameters of the system (4) are fixed to $a = 0.3$ and $b = 0.25$ by setting $R_{25} = 10$ kΩ and $G = 1.57$, and $\tau = 0.1$ is realized by selecting one APF with $R = 0.1$ kΩ. According to the changes of initial conditions ($x(0)$, $y(0)$, $z(0)$), Pspice simulations are made to the time-delayed system (4). It is obvious from Fig. 11 that the time-delayed system (4) has 13-scroll attractors within x varying in the interval [−36, 16] for initial conditions $(x(0), y(0), z(0)) = (0, 1, 0)$, while it has 11-scroll attractors within x varying in the interval [−8, 36] for initial conditions $(x(0), y(0), z(0)) = (0, 0, 1)$. Figure 12 confirms that the coexistence of multiple attractors with a variable number of scrolls can be observed in the time-delayed system (4).

5 Conclusion

In this paper, we have reported a time-delayed hyperchaotic system composed of multiscroll attractors with multiple positive LEs. Analytically, we predicted the values of time delay and system parameters of the time-delayed system (4) for which Hopf bifurcation would appear. The LEs spectrum of the time-delayed system (4) with different parameters varying is drawn. The

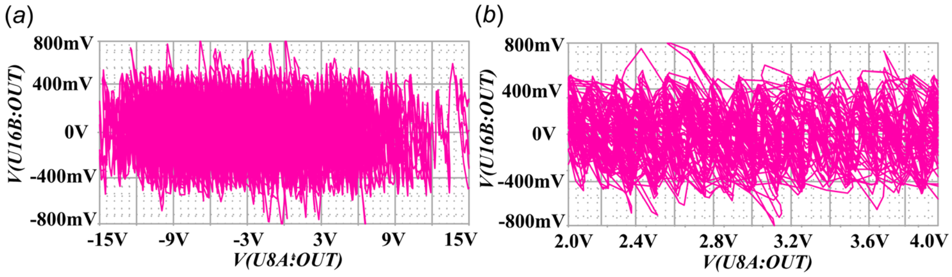

Fig. 9 Circuit simulations of hyperchaotic attractors with multiscroll of the time-delayed system (4) when initial conditions ($x(0)$, $y(0)$, $z(0)$) = (1, 1, 1): (*a*) hyperchaotic attractors and (*b*) local amplification of (*a*)

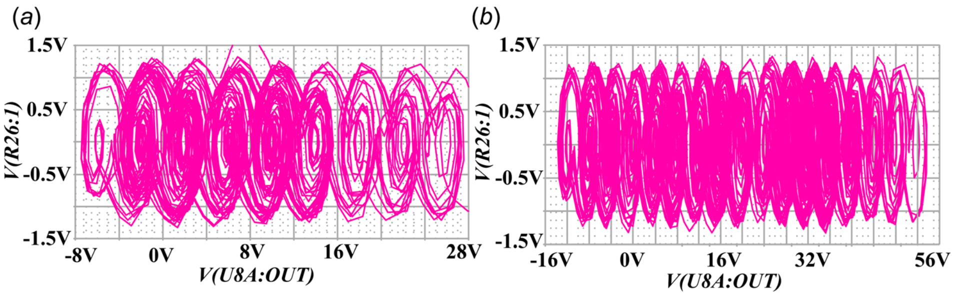

Fig. 10 Circuit simulations of multiscroll attractors of the nontime-delayed system (3) and the time-delayed system (4) when initial conditions ($x(0)$, $y(0)$, $z(0)$) = (1, 1, 1): (*a*) system (3) and (*b*) system (4) with $\tau = 0.1$

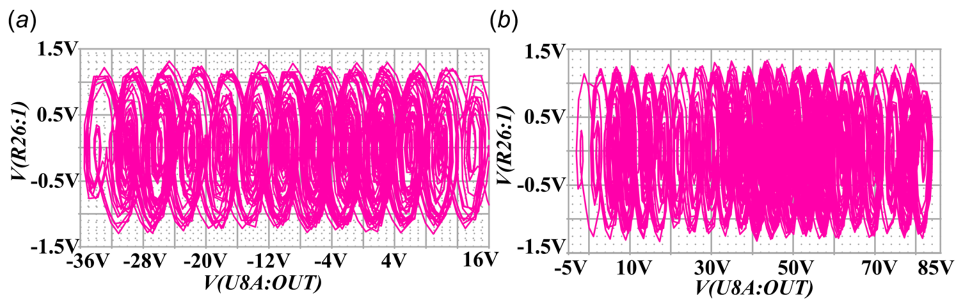

Fig. 11 Circuit simulations of different numbers of scrolls of the time-delayed system (4) when initial conditions ($x(0)$, $y(0)$, $z(0)$) = (0, 1, 0) and $t = 3000$: (*a*) $\tau = 0.1$, and (*b*) $\tau = 0.5$

presence of multiple positive LEs ensures the occurrence of hyperchaos in the time-delayed system (4). Apart from LEs, detailed numerical simulations proved that the dynamical characteristics of the time-delayed system (4) are far more complicated than those of the original system (3). The proposed time-delayed system (4) has been realized by electronic circuits, and its Pspice simulations are made. The analytical, numerical, and the experimental studies are in a good agreement, revealing the full system dynamical characteristics.

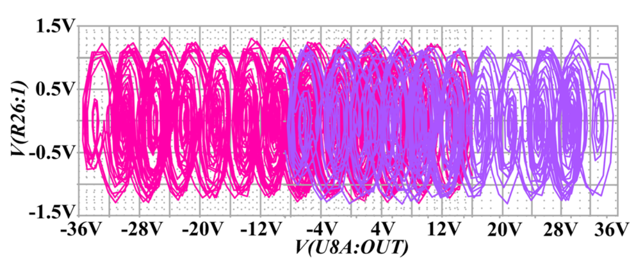

Fig. 12 Circuit simulations of coexistence of multiple attractors of the time-delayed system (4) when $\tau = 0.1$ and $t = 3000$: x varying in the interval [−36, 16] for initial conditions ($x(0)$, $y(0)$, $z(0)$) = (0, 1, 0) and the interval [−8, 36] for initial conditions ($x(0)$, $y(0)$, $z(0)$) = (0, 0, 1)

The following interesting features of the proposed three-order time-delayed system (4) are noticed, which may be important from the perspective of practical applications: (i) with the suitable choice of the system parameters, the time-delayed system (4) shows abundant dynamical behaviors, such as hyperchaos with multiple positive LEs, hyperchaotic attractors with multiscroll, Hopf bifurcation, limit cycle, and coexistence of multiple attractors. Thus, the proposed time-delayed system (4) can be used as an efficient chaotic or hyperchaotic generator for chaotic cryptography, chaos-based noise generator, and electronic communication applications. (ii) Moreover, since the chaotic and hyperchaotic oscillations of the time-delayed system (4) are well studied, further research can be carried out about the control and synchronization of the proposed system.

Acknowledgment

This work was supported by the National Natural Science Foundation of China (No. 61571185), The Natural Science Foundation of Hunan Province, China (No. 2016JJ2030), and the Open Fund Project of Key Laboratory in Hunan Universities (No. 15K027).

References

[1] Biswas, D., and Banerjee, T., 2016, "A Simple Chaotic and Hyperchaotic Time-Delay System: Design and Electronic Circuit Implementation," Nonlinear Dyn., **83**(4), pp. 2331–2347.

[2] Banerjee, T., and Biswas, D., 2013, "Theory and Experiment of a First Order Chaotic Delay Dynamical System," Int. J. Bifurcation Chaos, **23**(6), p. 1330020.

[3] Adhikari, B. M., Prasad, A., and Dhamala, M., 2011, "Time-Delay-Induced Phase-Transition to Synchrony in Coupled Bursting Neurons," Chaos, **21**(2), p. 023116.

[4] Banerjee, T., 2012, "Single Amplifier Biquad Based Inductor-Free Chua's Circuit," Nonlinear Dyn., **68**(4), pp. 565–573.

[5] Kye, W. H., Choi, M., Kurdoglyan, M. S., Kim, C. M., and Park, Y. J., 2004, "Synchronization of Chaotic Oscillators Due to Common Delay Time Modulation," Phys. Rev. E, **70**(4), p. 046211.

[6] Özkaynak, F., 2014, "Cryptographically Secure Random Number Generator With Chaotic Additional Input," Nonlinear Dyn., **78**(3), pp. 2015–2020.

[7] Andò, B., and Graziani, S., 2000, *Stochastic Resonance: Theory and Applications*, Kluwer Academic Publishers, Norwell, MA.

[8] Tamaševicius, A., Mykolaitis, G., and Bumeliene, S., 2006, "Delayed Feedback Chaotic Oscillator With Improved Spectral Characteristics," Electron. Lett., **42**(13), pp. 736–737.

[9] Srinivasan, K., Mohamed, I. R., Murali, K., Lakshmanan, M., and Sinha, S., 2011, "Design of Time Delayed Chaotic Circuit With Threshold Controller," Int. J. Bifurcation Chaos, **21**(3), pp. 725–735.

[10] Tamaševicius, A., Pyragiene, T., and Meškauskas, M., 2007, "Two Scroll Attractor in a Delay Dynamical System," Int. J. Bifurcation Chaos, **17**(10), pp. 3455–3460.

[11] Suykens, J. A. K., and Vandewalle, J., 1993, "Generation of n-Double Scrolls ($n = 1,2,3,4\ldots$)," IEEE Trans. Circuits Syst. I, **40**(11), pp. 861–867.

[12] Lü, J., Yu, S., Leung, H., and Chen, G., 2006, "Experimental Verification of Multidirectional Multiscroll Chaotic Attractors," IEEE Trans. Circuits Syst. I, **53**(1), pp. 149–165.

[13] Tang, W. K. S., Zhong, G. Q., Chen, G., and Man, K. F., 2001, "Generation of n-Scroll Attractors Via Sine Function," IEEE Trans. Circuits Syst. I, **48**(11), pp. 1369–1372.

[14] Yu, S., Lü, J., and Chen, G., 2007, "A Module-Based and Unified Approach to Chaotic Circuit Design and Its Applications," Int. J. Bifurcation Chaos, **17**(5), pp. 1785–1800.

[15] Yu, S., Lü, J., Leung, H., and Chen, G., 2005, "Design and Implementation of n-Scroll Chaotic Attractors From a General Jerk Circuit," IEEE Trans. Circuits Syst. I, **52**(7), pp. 1459–1476.

[16] Lin, Y., Wang, C., and Zhou, L., 2016, "Generation and Implementation of Grid Multiscroll Hyperchaotic Attractors Using CCII+," Optik, **127**(5), pp. 2902–2906.

[17] Yu, S., and Tang, W. K. S., 2009, "Generation of $n \times m$-Scroll Attractors in a Two-Port RCL Network With Hysteresis Circuit," Chaos, Solitons Fractals, **39**(2), pp. 821–830.

[18] Sprott, J. C., 2000, "Simple Chaotic Systems and Circuits," Am. J. Phys., **68**(8), pp. 758–763.

[19] Sprott, J. C., 2000, "A New Class of Chaotic Circuit," Phys. Lett. A, **266**(1), pp. 19–23.

[20] Yalçin, M. E., 2007, "Multi-Scroll and Hypercube Attractors From a General Jerk Circuit Using Josephson Junctions," Chaos, Solitons Fractals, **34**(5), pp. 1659–1666.

[21] Ruan, S., and Wei, J., 2001, "On the Zeros of a Third Degree Exponential Polynomial With Applications to a Delayed Model for the Control of Testosterone Secretion," Math. Med. Biol., **18**(1), pp. 41–52.

[22] Hale, J., and Lunel, S. M. V., 1993, *Introduction to Functional Differential Equations*, Springer Verlag, New York.

[23] Farmer, J. D., 1982, "Chaotic Attractors of an Infinite-Dimensional Dynamical System," Physica D, **4**(3), pp. 366–393.

[24] Benettin, G., Galgani, L., Giorgilli, A., and Strelcyn, J. M., 1980, "Lyapunov Characteristic Exponents for Smooth Dynamical Systems and for Hamiltonian Systems; A Method for Computing All of Them. Part 1: Theory," Meccanica, **15**(1), pp. 9–20.

[25] Shampine, L. F., and Thompson, S., 2001, "Solving DDEs in MATLAB," Appl. Numer. Math., **37**(4), pp. 441–458.

[26] Wang, Q., Yu, S., Li, C., and Lü, J., 2016, "Theoretical Design and FPGA-Based Implementation of Higher-Dimensional Digital Chaotic Systems," IEEE Trans. Circuits Syst. I, **63**(3), pp. 401–412.

[27] Ojoniyi, O. S., and Njah, A. N., 2016, "A 5D Hyperchaotic Sprott B System With Coexisting Hidden Attractors," Chaos, Solitons Fractals, **87**, pp. 172–181.

[28] Li, C., and Sprott, J. C., 2014, "Coexisting Hidden Attractors in a 4-D Simplified Lorenz System," Int. J. Bifurcation Chaos, **24**(3), p. 1450034.

[29] Ma, J., Wu, X., Chu, R., and Zhang, L., 2014, "Selection of Multi-Scroll Attractors in Jerk Circuits and Their Verification Using Pspice," Nonlinear Dyn., **76**(4), pp. 1951–1962.